

VHDL-AMS BASED MODELING OF SIC-SCHOTTKY DIODE

Tarek SELMI

Australian College of Kuwait, Kuwait, West Mishref Mubarak Al-Abdullah Al-Jaber Area - Al Aqsa Mosque Street

Phone: +965 25376111 Fax: +965 25376222, Email: t.selmi@ack.edu.kw

Mohamad SABATI

Australian College of Kuwait, Kuwait, West Mishref Mubarak Al-Abdullah Al-Jaber Area - Al Aqsa Mosque Street

Phone: +965 25376111 Fax: +965 25376222, Email: m.sabati@ack.edu.kw

Otmar IRSHEID

Australian College of Kuwait, Kuwait, West Mishref Mubarak Al-Abdullah Al-Jaber Area - Al Aqsa Mosque Street

Phone: +965 25376111 Fax: +965 25376222, Email: o.irscheid@ack.edu.kw

Hania BAITIE

Australian College of Kuwait, Kuwait, West Mishref Mubarak Al-Abdullah Al-Jaber Area - Al Aqsa Mosque Street

Phone: +965 25376111 Fax: +965 25376222, Email: h.baitie@ack.edu.kw

Abstract: *Over the last few decades, several work has been done on behavioral models and simulation tools. However, there is always some space for improvements and enhancements for previous work. The VHDL-AMS language makes possible the description of semiconductor devices based on mathematical equations. Moreover, VHDL-AMS is a useful tool for the analog design community. Also, the efficient semiconductor device models must be investigated in order to finely predict and extract its technological and electrical parameters. In this sense, the authors in this paper demonstrate the potential merits of the VHDL-AMS in the field of modeling of a SiC power Schottky diode. The diode's analytical model and its working principles are presented in this paper. This is carried out by taking into account the technological and electrical effects with VHDL-AMS, and with relevant parameters hitting a deep match between the simulated characteristics of the VHDL-AMS model and the measured characteristics of the SiC Schottky diode.*

Key words: *Semiconductor device doping, VHDL-AMS, Simulation, Behavioral model, Analytic Model, Static response, Transient response, Silicon Carbide, Schottky diode.*

1. Introduction

Following the renovation made in the technology sector in recent decades, several semiconductor devices have emerged for its application in power electronics. The quality that the industry is seeking is at the physical performance limits. Until now, the semiconductors' market is still dominated by the silicon type. The exceptional quality of such material, associated to the huge effort of the industry, has made from silicon the material that covers nearly all the requirements of the power electronics needs. Nevertheless, the increase of requirements from performance viewpoint has reached and perhaps

exceeded those offered by the silicon type, hence reaching a limit.

Semiconductor devices find numerous applications in the industry where better performance is sought. Such performance is represented by but not limited to voltage drops under low forward bias in order to reduce losses for a given high current and high breakdown voltage all along with a quick switching behaviour to justify the ability of a proper working under high frequencies.

From another side of view and performing under severe temperature conditions; the silicon carbide (SiC) is considered the best candidate for the power electronic devices [1, 2, 3]. Silicon carbide is known as one of the best performance wide band gap materials. It is known for its small, fast and better performance characteristics [4].

In light of the above, the excellent properties of the SiC from one hand, and the requirements of the market from the other hand have motivated recent research trends to be toward putting a particular emphasis on modelling and characterizing such semiconductor material [5].

Typically, modelling of a power semiconductor device can be either based on semiconductor equations within circuit simulators such as SABER, PACTE, SIMPLORER and others [6], or on finite elements simulators such as DESSIS and MEDICI. Moreover, most models are based on the classical approaches implemented in PSpice simulator which builds on an equivalent circuit that represents the electrical behaviour of that particular device. Otherwise, the idea is to directly solve the semiconductor equations. Evidently, this latest method allows to a fine studying of the physics as well as the behaviour of the device. In fact, the designer should be able to predict the performance of his device and to provide models allowing the exploitation of the parameters of the entire

circuit.

In light of that, behavioural models seem evidently to be able to respond to such expectations. Such models can be coded using numerous programming languages such as VHDL-AMS, Verilog, C and C++.

However, it seems judicious to highlight a language allowing a simple interface with behavioural numerical models. That is why, VHDL-AMS has been judged as the most appropriate tool to model the SiC Schottky diode within the frame of this work.

2. Model Analysis

The PN junction is the origin of all semiconductors. Considering a P+N abrupt and asymmetric junction, the positive charge at the space charge zone is given as [7,8]:

$$Q_j = Aqx_e N_D \quad (1)$$

Where A is the total surface area of the diode.

The space charge zone extends in the less-doped region (N) if we assume that the electric field is null at this zone.

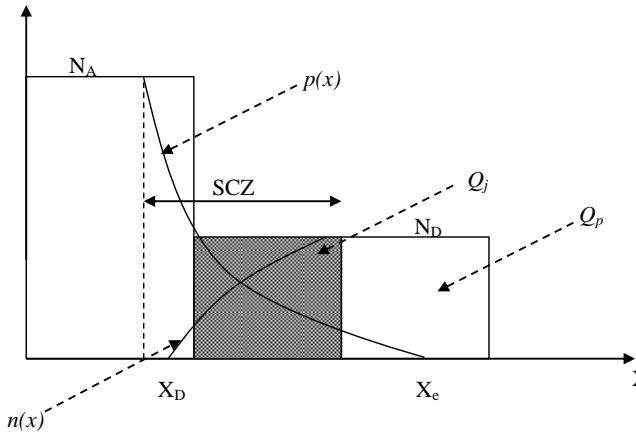


Fig. 1. Doping and concentrations of an abrupt junction.

The integral of the Poisson's equations leads to the potential flux ψ as a function of the abscissa x [9]. The barrier height of the junction is given as:

$$U_B = \psi(X_D) - \psi(X_e) = \frac{Q_j^2}{2q\epsilon_s N_D A^2} \quad (2)$$

Equations (1) and (2) give:

$$X_e = \sqrt{\frac{2\epsilon_s U_B}{qN_D}} \quad (3)$$

Based on (2), we can write:

$$Q_j = A\sqrt{2\epsilon_s N_D} \sqrt{U_B} \quad (4)$$

If we consider that the concentration of holes at zone N is much less than the doping, the diffusion equation of holes at the static regime can be written as:

$$\frac{dQ}{dt} = \mu_p \mu_T \frac{d^2 P}{dx^2} - \frac{P - P_0}{\tau_P} \quad (5)$$

Where $P_0 = \frac{n_i^2}{N_D}$ is the concentration of minors at

the equilibrium, and τ_P and μ_p are the lifetime and mobility of holes respectively which is assumed to be constant.

The Boltzmann's constant gives the concentration of holes at the right limit of the space charge zone:

$$p(x, t) = p_1 = N_A \exp\left(-\frac{U_B}{U_T}\right) \quad (6)$$

Besides, if we assume that the neutral zone N is as wide as holes can recombine before reaching the right limit of the SCZ, the simplest variational approximation that satisfies the static solution might be written as the following form:

$$\approx p(t, x) = p_0 + (p_1(t) - p_0) \exp\left(-\frac{x}{L_{Dp}}\right) \quad (7)$$

Where $L_{Dp} = \sqrt{\mu_p \mu_T \tau_P}$ is the length of the diffusion of holes.

The total charge in excess of the holes is calculated by the following relationship [10]:

$$Q_p = qA \int_{X_e}^{\infty} (p - p_0) dx \quad (8)$$

Thus,

$$Q_p = I_D \tau_P = qAL_{Dp} (p - p_0) \quad (9)$$

The voltage drop across the diode is:

$$V_d = V_j - U_B \quad (10)$$

Where $V_j = U_T \ln\left(\frac{N_D N_A}{ni^2}\right)$ is the construction

voltage of the junction. It represents the voltages drops across the metal-semiconductor junction.

By combining (6), (9) and (10), the following equation can be written as:

$$I_D = I_s \left(\exp \left(\frac{V_d}{U_t} \right) - 1 \right) \quad (11)$$

Where $I_s = \frac{qAni^2 \mu_p \mu_T}{N_D L_{Dp}}$ is the diode's

saturation current.

The equivalent schematic of the diode can be represented as follow:

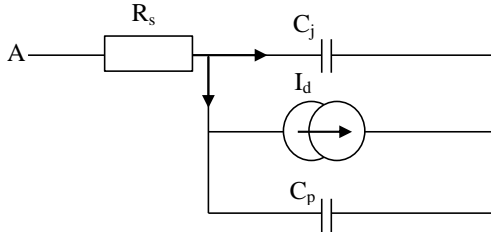


Fig. 2. Equivalent circuit of the diode.

The resistance R_s takes into account the different voltage drops (access to the junction).

The positive charge Q_j is represented by the electric capacitance C_j and is defined by the following equation:

$$\frac{dQ_j}{dt} = \frac{dQ_j}{dU_B} \frac{dU_B}{dt} = \frac{dQ_j}{dV_d} \frac{dV_d}{dt} = C_j \frac{dV_d}{dt} \quad (12)$$

That is to say:

$$C_j = \frac{A}{2} \sqrt{\frac{2\epsilon_s q N_D}{V_j}} \frac{1}{\sqrt{1 - \frac{V_d}{V_j}}} \quad (13)$$

In general, the expression of the capacitance C_j is given by the following:

$$C_j = C_{j0} \left(1 - \frac{V_d}{V_j} \right)^{-m} \quad (14)$$

Where m is the gradual coefficient which is equal to 1/2 for an abrupt junction and 1/3 for a gradual junction [11].

The excess positive charge Q_p stocked at the neutral zone is represented by means of the electric capacitance C_p given by:

$$\frac{dQ_p}{dt} = I_p - I_D = \tau_p \frac{dI_D}{dt} = \frac{dI_D}{dV_d} \frac{dV_d}{dt} = C_p \frac{dV_d}{dt} \quad (15)$$

Where $C_p = \tau_p \frac{dI_D}{dV_d}$

The forward current I_D is represented by a non-linear current source. The SPICE model takes into account the recombination phenomenon through an empirical parameter N called emission coefficient. Hence, the direct current of the diode is given as:

$$I_D = I_s \left(\exp \left(\frac{V_d}{N V_t} \right) - 1 \right) \quad (16)$$

In light of the above analysis and mathematical modulation, the VHDL-AMS model was experimentally studied in this study.

Since 2001, numerous semiconductor manufactures (Infineon, Microsemi & Gree, Fairchild,...) started proposing their catalogues containing silicon carbide (SiC) Schottky diode as described in the table 1 [12].

TABLE I

SiC POWER SEMICONDUCTOR TIMETABLE

Year	Event
2001	First SiC Schottky diode introduced to the market
2004-2005	Cree Started the production of 4" SiC wafer
2006-2007	First SiC JFET Sold in low volumes
2007	Hybrid SiC power module launched
fall 2008	Semi-South releases first N-Off SiC FET, TranSiC launch SiC BJT
end 2008	Full SiC power module introduced to the market
2009	4 inch SiC wafer costs drop to \$1.500
2010-2011	ROHM SiC MOSFET in production
2011	Cree SiC MOSFET introduced to the market
fall 2012	Infenion announces 1200V CoolSiC JFET
end 2012	Cree launches 6 inch SiC wafer mass production
fall 2013	Devices mass produced on 6" wafers appear

In this paper, we have chosen the SiC Schottky diode SDB6S60 of Infineon technologies. Within the frame of this work, it was decided to estimate the technological and electrical parameters of the SPICE model of the above mentioned diode. To extract such parameters, several tests on $I(V)$ and $C(V)$ were done. To be able to do so, it was mandatory to know the effective surface of the diode.

Classically, a simple inspection of the diode's chip might give an initial value of the effective surface of the diode. However, we could obtain an optimal value of such surface based on the current density given by the manufacture in the datasheet following the law:

$$A_{op} = \frac{I_F}{J}$$

Thus, the surface was found equal to $1.2\mu\text{m}^2$.

The effective surface as well as other parameters of the diode such as the doping N_D of the weakly doped zone and the width W of such zone will be identified and validated using a method originally developed in 1998 by Ghedira [13]. Such method helps to extract N_D , W , and A based on the analysis of the transient signals of two to three reverse commutations starting from the resting state. Accordingly, a VHDL-AMS model was developed to verify the simulated waves with the experimental ones.

3. Static Forward Behavioral Analysis

The classic measurement method $I(V)$ and $C(V)$ have permitted to determine the parameters of the static responses at 300K.

The curves $I(V)$ were done using TEKTRONIX drawers 370 and 371 while curves $C(V)$ were done using an RCL-meter HP4284A.

The classic measurement method $I(V)$ and $C(V)$ have permitted to determine the following parameters of the static responses at ambient temperature 300K:

- Series resistance: $390\text{m}\Omega$
- Ideality coefficient: $n=1.028$.
- Saturation current: $I_s=1.175 \text{ E-}16 \text{ A}$
- Barrier Schottky extracted from $I(V)$: $\phi_e=1.2\text{eV}$.
- Epitaxial thick: $2.5\mu\text{m}$.
- Epitaxial doping $N_D=1.2\text{E}16\text{cm}^3$.

Figure 3 represents the $I(V)$ curve in forward bias at the ambient temperature. It helps to find the ideality factor n given by:

$$n = \frac{q}{KT} \left(\frac{d(\ln[I])}{d(V)} \right)^{-1}$$

and the barrier height given by:

$$\phi_e = -\frac{KT}{q} \ln \left(\frac{I_{sat}}{A^* T^2 S} \right)$$

Where:

I_{sat} : Exponential [ordinate at the origin ($\ln(I)=f(V)$)].

$A^*=A.\mu\text{m}^2$ (0.763 for the SiC-4H).

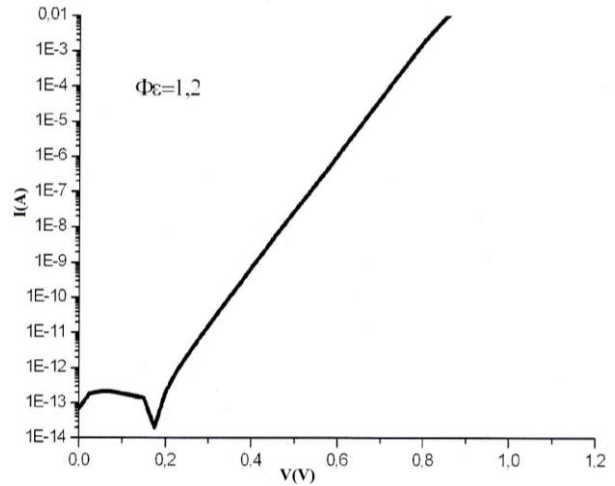


Fig. 3. Measured $I(V)$ of the SiC diode SDB6S60 in order to estimate the ideality factor.

Figure 4 shows the forward characteristic of the SiC diode, drawn in SWEEP mode using TEKTRONIX 371. It helps to estimate the value of the dynamic resistance to $390\text{m}\Omega$. Such value is taken as the series resistance of the diode. It is given as:

$$R_s = \left(\frac{dI}{dV} \right)^{-1}$$

The above resistance can be assimilated to the resistance of the epitaxial layer + the resistance of the

substratum, that is to say: $R_{sub} = \rho \frac{W_{sub}}{S_{chip}}$

And

$$R_s = R_{sub} + \frac{1}{N_D q \mu} \frac{W_{epi}}{S}$$

Therefore, the width of the epitaxial zone is given as follow:

$$W_{epi} = S(R_s - R_{sub})N_D q \mu$$

Where W_{sub} and S_{chip} are provided in the datasheet, S is the surface and μ is $800\text{cm}^2/\text{Vs}$.

The width of the epitaxial zone W_{epi} is around $2.5\mu\text{m}$.

The doping is estimated from the curve $C(V)$ measured using the HP4284A. Its expression is given by the following relationship:

$$N_D = \frac{2}{s^2 q \epsilon_r \epsilon_0 \frac{d\left(\frac{1}{C^2}\right)}{d(V)}}$$

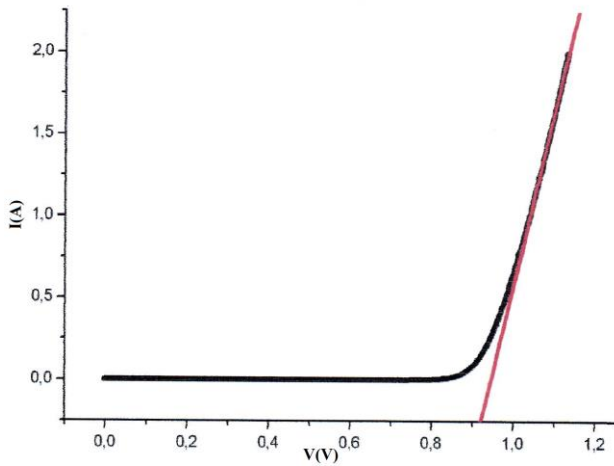


Fig. 4. Measured $I(V)$ of the SiC diode SDB6S60 in order to estimate the series resistance.

As a result of the above analysis and explanation, the experimental curve of figure 5 helps to find out a doping N_D of $1.2 \text{ E}16 \text{ cm}^{-3}$.

4. TRANSIENT REVERSE BEHAVIORAL ANALYSIS

The idea now is to develop an analytical VHDL-AMS model of the SiC Schottky diode based on the SPICE model. Such model, implemented using the simulator SIMPLORER, helps to draw the transient curves of the reverse bias of the diode at the thermodynamic equilibrium. The electric parameters of the diode estimated previously by the classic method will be considered as the initial values used within VHDL-AMS. Such parameters are respectively the effective surface A , N_D , and W of the diode.

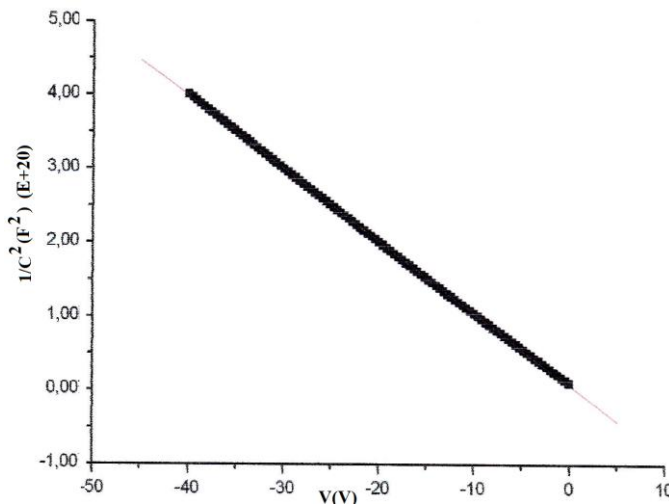


Fig. 5. Measured curve derived from $C(V)$ of the SiC diode SDB6S60 in order to estimate the doping N_D .

To do so, we have developed an experimental test bench in order to measure the transient characteristics of the diode in the reverse switching mode starting

from the resting state.

Starting from the previously mentioned characteristics, we can plot the maximum reverse voltage V_{RM} as a function of the applied voltage V_R , the maximum reverse current I_{RM} as a function of V_R and the reverse recovery time t_{RR} as a function of V_R . Figure 6 shows the simulated curves in transient mode of the SiC diode SDB6S60 using VHDL-AMS.

In reference to the simulated characteristics, we have defined the transient parameters of the diode as follow:

- I_{RM} : The maximum reverse current.
- V_{RM} : The maximum reverse voltage.
- t_{RR} : The reverse recovery time.
- dV_F/dt : Slope of the reverse voltage at the moment of passing to I_{RM} .
- dI_F/dt : Slope of the recovery current at the moment of passing to V_{RM} .

Figure 7 shows the test bench realized and curves given by figures 8 and 9 have been compared to those plotted from the VHDL-AMS model in order to estimate with high precision the technological parameters of the diode.

The given capacitance of the junction for a voltage equal to zero is $C_{j0}=300 \text{ pF}$ and the gradual coefficient of the junction is $m=0.33$.

Based on those parameters as well as on the simulation MEDICI, we have identified the technological parameters of the SiC-Schottky diode for an inductance of $1.5 \mu\text{H}$.

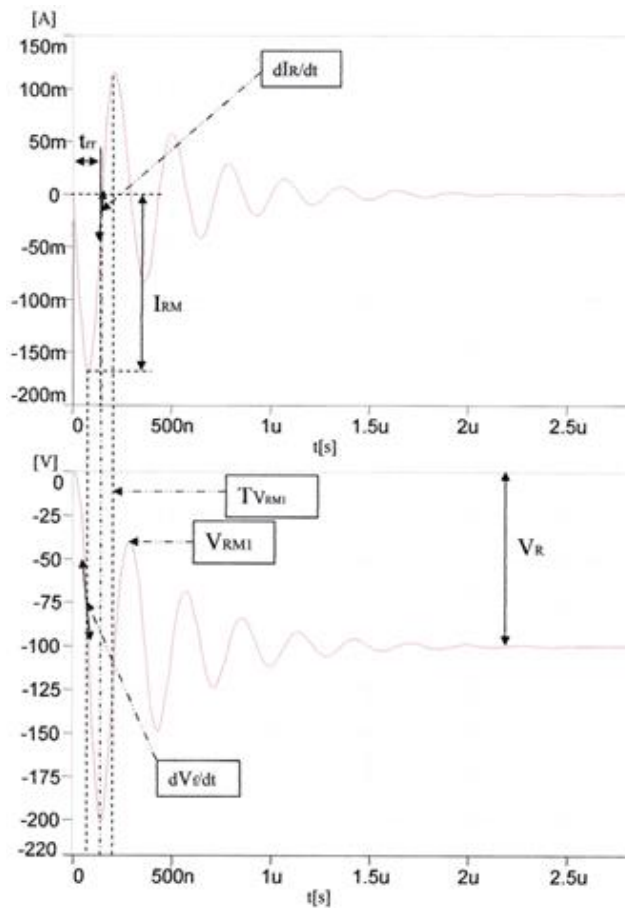


Fig. 6. Simulated curves of the SiC diode SDB6S60, from top to bottom: $I(t)$ and $V(t)$.

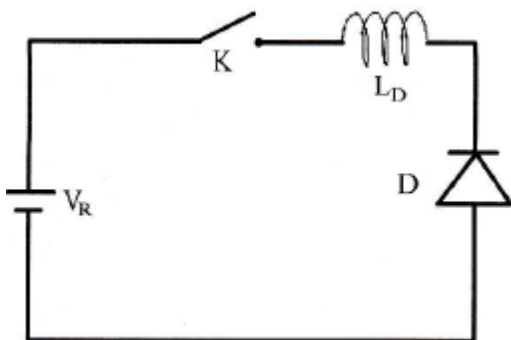


Fig. 7. Realized test bench for the transient analysis.

With regards to the plotted characteristics (simulated and measured), a comparison has been done in figures 8 and 9 and electrical as well as technological parameters of the investigated SiC diode have been extracted. In regards to the experimental results, two different techniques that complement each other have been used. The first is classical to study the static behaviour of the diode while the second is transient to figure out the technological and electrical parameters of the given diode.

The comparison between simulated and measured characteristics has led to a good match which leads to

the extraction the real parameters of the SiC diode SDB6S60.

The effective surface of the diode was found to be equal to $1.19 \mu\text{m}^2$. The doping is $1.23\text{E}+16 \text{ cm}^{-3}$ and the width of the zone weakly doped zone is $W=2.56 \mu\text{m}$.

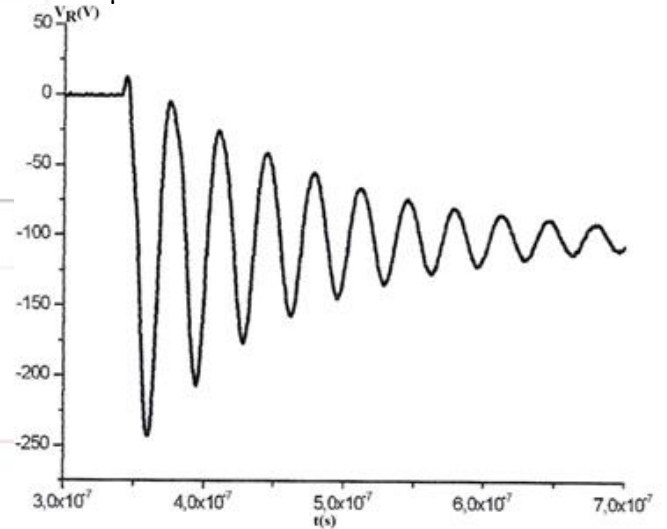


Fig. 8. Measured reverse voltage V_R as function of time of the SiC diode SDB6S60.

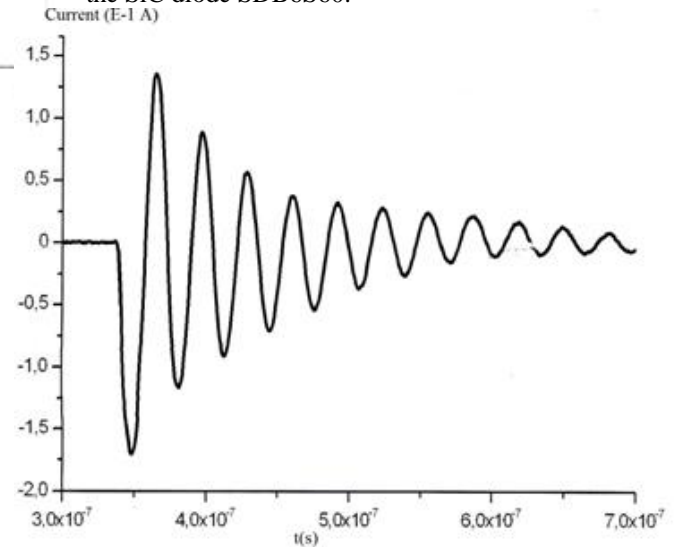


Fig. 9. Measured reverse current I_R as function of time of the SiC diode SDB6S60.

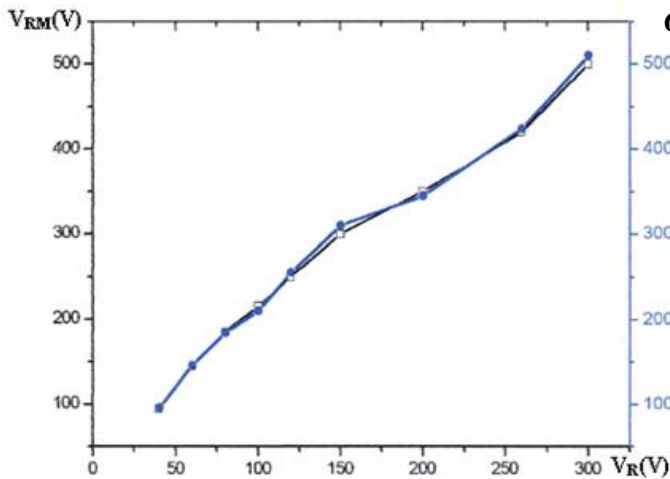


Fig. 10. Comparison of simulated and measured reverse voltage V_{RM} of the SiC diode SDB6S60 (Blue: Simulation, Black: Measurement).

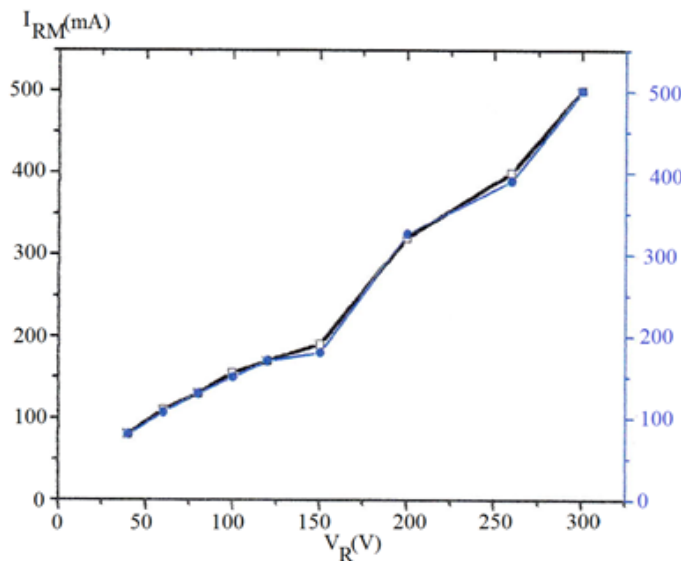


Fig. 11. Comparison of simulated and measured reverse current I_{RM} of the SiC diode SDB6S60 (Blue: Simulation, Black: Measurement).

5. CONCLUSION

This paper deals with a VHDL-AMS model of a SiC Schottky diode. The simulated results either in the static or in the transient domains were validated by means of experimental results. The VHDL-AMS model was based on mathematical equations that describe the behaviour of the schottky diode. In light of the above, the extraction of real parameters of the SiC diode SDB6S60 has been achieved; hence, providing the industry a better knowledge about the SiC to be a crucial alternative for the power electronic devices.

6. REFERENCES

1. A.Elasser, M. H. Kheraluwara, M. Ghezzi, R.L. Steigerwald, N.A.Evers, Kretchmer James and T.P. Chow, "A comparative evaluation of new silicon carbide diodes and state-of-the-art silicon diodes for power electronic applications," *IEEE Trans. On Industry Applications*, vol. 39, pp. 915-921, Aug. 2003.
2. J. Rabkowski, D. Peftitsis and H.P. Nee, "Silicon Carbide Power Transistors: A New Era in Power Electronics Is Initiated," *IEEE Magazine of Industrial Electronics*, vol. 6, pp. 17-26, June 2012.
3. Hui Zhang, and L.M. Tolbert, "Efficiency Impact of Silicon Carbide Power Electronics for Modern Wind Turbine Full Scale Frequency Converter," *IEEE Trans. on Industrial Electronics*, vol. 58, pp. 21-28, Jan. 2011.
4. U.S. Department of Energy, "Energy Efficiency and Renewable Energy", April 2013
5. N. Ericson, S. Frank, C. Britton, L. Marilino, Sei-Hyung Ryu, D. Grider, A. Mantooth, M. Francis, R. Lamichhane, M. Mudholkar, P. Shepherd, M. Glover, J. Valle-Mayorga, T. McNutt, A. Barkley, B. Whitaker, Z. Cole, B. Passmore and A. Lostetter, "A 4H Silicon Carbide Gate Buffer for Integrated Power Systems," *IEEE Trans. on Power Electronics*, vol. 29, pp. 539-542, Feb. 2014.
6. T.R. McNutt, A.R. Hefner, H.A. Mantooth, D. Berning and Sei-Hyung Ryu, "Silicon Carbide Power MOSFET Model and Parameter Extraction Sequence," *IEEE Trans. on Power Electronics*, vol. 22, pp. 353-363, March 2007.
7. S. M. Sze, *Physics of Semiconductor Devices*, vol. I New York: John Wiley & Sons, 1981, Ch. 2.
8. E. Gwynne, "The Poisson Integral Formula and Representations", *Rose-Hulman Undergraduate Mathematics Journal*, vol 12, no. 2, Fall 2011
9. Backes and U. Schmid, "Impact of doping level on the metal assisted chemical etching of p-type silicon", *Science Direct*, vol. 193, pp.883-887, March 2014,
10. Grebennikor, N. Sokal, and M.J. Franco, "Switchmode RF and Microwave Power Amplifiers", Elsevier, 2nd ed. 2012.
11. S. M. Sze, *Semiconductor Devices: Physics and Technology*, vol. II New York: John Wiley & Sons, 2002.
12. Richard Eden, *Market Forecasts for Silicon Carbide & Gallium Nitride Power Semiconductors*. [Online]. Available: <http://www.apec-conf.org/wp-content/uploads/2013/09/is1.4.2.pdf>.
13. S. Ghedira, "Contribution à l'estimation des paramètres technologiques de la diode PIN de puissance à partir des résultats expérimentaux," Ph.D. dissertation, Dept. Elec. Eng., INSA-ISAL 29, 1998